THE UNIVERSITY OF MICHIGAN

INDUSTRY PROGRAM OF THE COLLEGE OF ENGINEERING

ANALYSIS OF POWER SPINNING OF CONES

B. Avitzur
C. T. Yang

November, 1959

IP-402

VMR0152

ACKNOWLEDGMENT

Assistance from Mr. Serope Kalpakcioglu of the Cincinnati Milling Machine Company and staffs in Spincraft, Inc. in obtaining the experimental data is deeply appreciated.

NOMENCLATURE

$\dot{w}$ = rate of work or energy of deformation per unit volume in $\frac{\text{in-lb}}{\text{in.}^3 \text{ min.}}$

$\dot{W}$ = total energy of deformation

V = volume under the roller

$\bar{\sigma}$ = effective stress

$\dot{\bar{\phi}}$ = effective strain rate

R, θ, Z = polar coordinate directions of the spun cone

$\dot{\varepsilon}$ = strain rate

$\dot{\varepsilon}_{RR}$, $\dot{\varepsilon}_{\theta\theta}$, $\dot{\varepsilon}_{ZZ}$ = normal strain rates in R, θ and Z directions

$\dot{\varepsilon}_{R\theta}$, $\dot{\varepsilon}_{\theta Z}$, $\dot{\varepsilon}_{ZR}$ = shear strain rates

U_R, U_θ, U_Z = velocities in R, θ, and Z directions

N = rotating speed of the cone, in revolutions per minute

$\dot{\varepsilon}_{ij}$ = strain deviator tensor

S_{ij} = stress deviator tensor

$\frac{1}{\mu}$ = modulus of plasticity

$\dot{e}$ = hydrostatic strain rate

$\dot{e}_{ii}$ = summation of three principal strain rates = $\dot{e}_{11} + \dot{e}_{22} + \dot{e}_{33}$

X, Y, Z = rectangular coordinate directions of the spun cone

k = yield limit in shear = $\frac{\sigma_o}{\sqrt{3}}$

σ_o = yield limit in tension

S_{RZ}, $S_{Z\theta}$, $S_{\theta R}$ = deviator shear stresses

τ_{RZ}, $\tau_{Z\theta}$, $\tau_{\theta R}$ = total shear stresses

σ_{ij} = total stress tensor

S = hydrostatic stress tensor

δ_{ij} = unit tensor

s = surface area

s_o = initial thickness of blank

α_o = 1/2 included angle of the cone

n = number of revolutions

r_o = radius of the round-off of the roller

x, y, z = coordinate directions for roller, z in the direction of feed, F; x in the direction normal to the cone surface; y is normal to xz plane

F = feed of roller (in/rev)

R_o = instantaneous radius at which the roller touches the cone

ρ_o = radius of the torus on the roller

T = time passed from the starting point

t = tangential force

$\dot{W}_T$ = tangential power

$\dot{W}_F$ = feed power

γ = shear strain

ξ = shear deformation

$\dot{W}^o$ = power consumption to deform the cone in experimental tests, assumed equal to $\dot{W}$

T_o = starting time

$\dot{W}'$ = weighted power = $\dfrac{\dot{W}\sqrt{3}}{\sigma_o s_o N}$

t' = weighted tangential force = $\dfrac{t}{s_o \sigma_o}$

INTRODUCTION

Spinning is generally a cold working process in which a rotating disk of sheet metal is deformed into a cup or cone by applying a localized pressure to the outside of the disk with a simple round-ended wood or metal stick. In common spinning practice the disk is deformed against a pattern having the final shape of the desired product. A very skillful machinist could, however, spin-form a cup or cone with no pattern-support at all. In these conventional types of spinning the thickness of the sheet metal is practically unchanged.

In the last few years a new type of spinning called "shear spinning" was developed. It has also other names, such as "power spinning," "flow-turning" or "roll-forming." Essentially they mean the same operation. In this process the work is done on a machine having the pattern and blank attached onto the spindle as usual but the metal was deformed by a roller which is mechanically operated (see Fig. 1). Moreover, in this operation the radial distance at any point on the cone remains the same before and after spinning and the thickness is therefore bound to be changed. This process has been widely used in making television picture-tube cones, etc.

Previous researchers[1] have done some work on the analysis of power, forces and stresses involved in this problem. But they are all limited to a certain extent. The authors attempted to study the problem in more detail--first with analytical approach and then the results were checked by experimental tests.

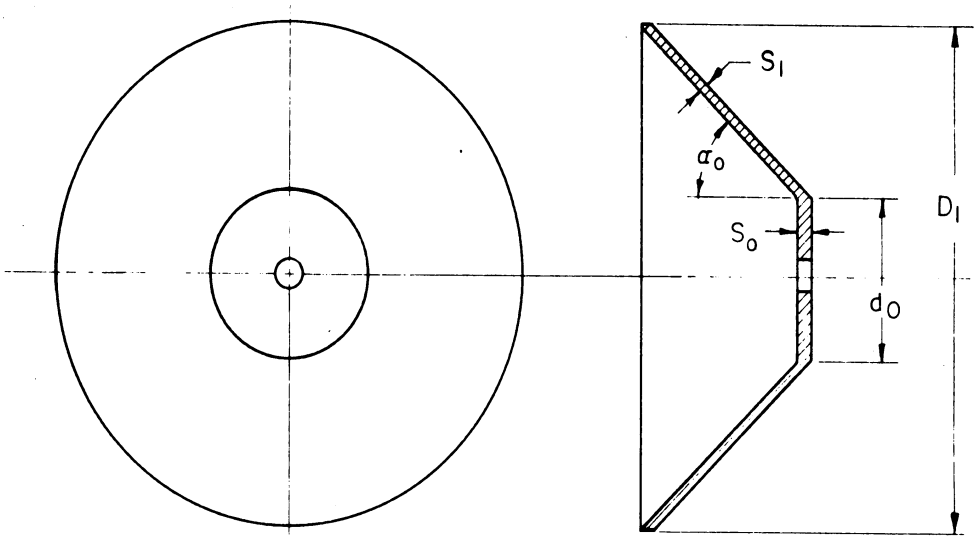

THE FINISHED CONE

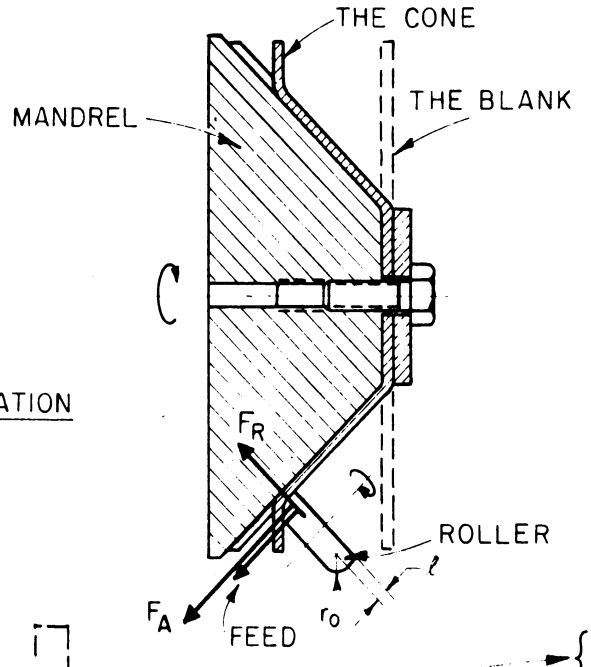

THE OPERATION

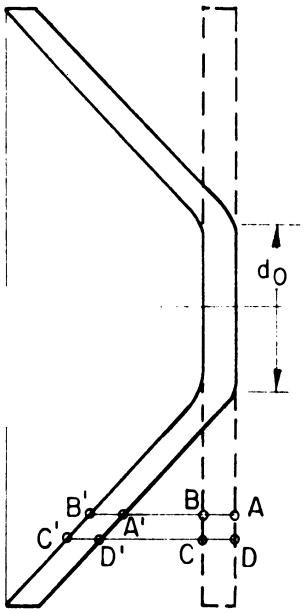

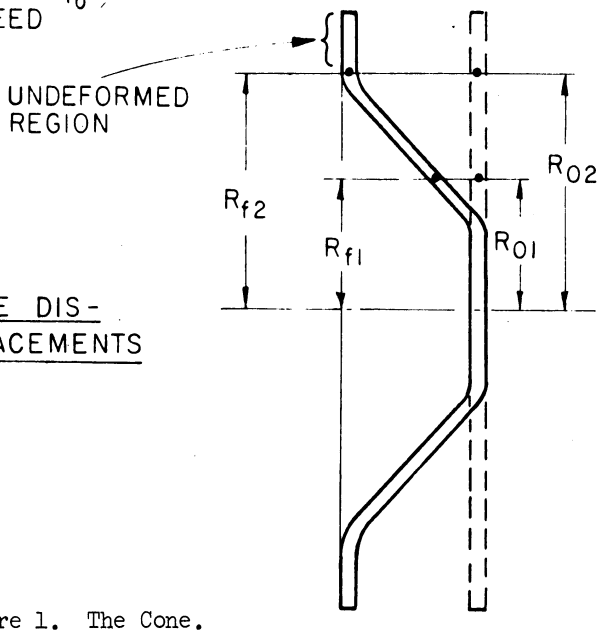

THE DIS-PLACEMENTS

Figure 1. The Cone.

THE NATURE OF DEFORMATION OF METAL IN THE PROCESS

A sheet metal blank in power spinning could be deformed by a process of bending, shearing or a combination of both (see Fig. 2). In bending the radial distance of any point at mid-thickness of the cone (point o or s in Fig. 2) remains unchanged. The lines AB and CD in Fig. 2 remain straight and normal to the surfaces. Therefore, the thickness before and after spinning can be related by the following equation:

$$\text{Thickness } A'B' = \text{Thickness } AB \cdot \sin\alpha_0$$

In shearing, however, not only points at mid-thickness but any material point have the same radial distance before and after deformation. The straight lines AB and CD in lower half of Fig. 2 change to $A'B'$ and $C'D'$ but remain parallel to the Z axis. Besides, $AB = A'B'$ and $CD = C'D'$; thus thickness after deformation = (thickness before deformation)$\cdot \sin\alpha_0$.

From the experimental tests described later it was found that the actual deformation pattern is a combination of bending and shearing. However, for the case of small included angles of a spun cone, the deformation is close to pure shear. Also for the sake of simplicity the pure shear deformation is assumed in the following analysis.

THE ANALYSIS

In the analysis the following assumptions were made:

1. Mises material is used, which implies that:
   (a) the material is homogeneous and isotropic,
   (b) there is no elastic deformation, and consequently no volumetric change,
   (c) there is no strain hardening.
2. The thickness of the blank is much smaller than the minimum radius of the cone.
3. The metal deforms under the roller in pure shear.

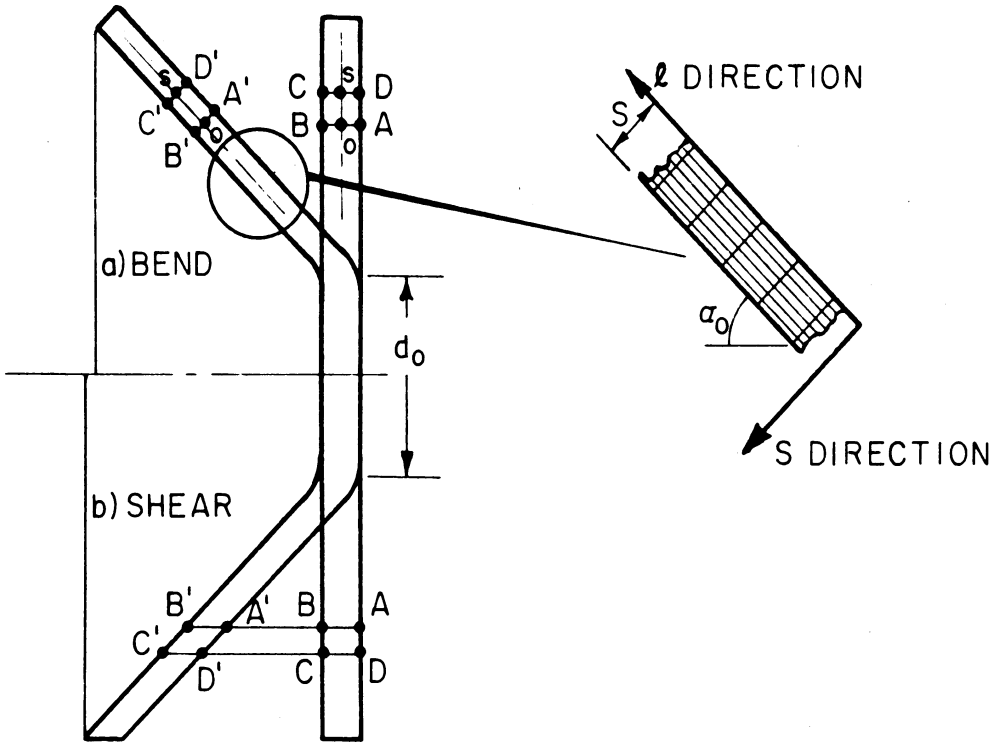

Figure 2. The Shear and Bending Strains.

4. The frictional force under the roller is neglected. This is justified, because the relative velocity between the cone and the roller is very small. Also this was substantiated by a previous publication by Reichel[2] which states that lubricants do not affect the force.

It was observed in the actual process and thence followed in the analysis that metal deforms instantaneously underneath the roller. The rest of the cone is strain free at the instant. From a variety of roller shapes, as shown in Fig. 3, shape I was chosen to be analyzed. The roller is assumed to have its axis parallel to the side of the cone. The choice of the coordinate axes XYZ with the origin at O is indicated in Fig. 4. Another set of cylindrical polar coordinates (R,θ,Z) with the same origin and Z axis as in XYZ coordinates was introduced. The assumed shear strain field is also illustrated in the lower part of Fig. 4. In the analysis the "Deformation Energy" theory was used which is indicated as follows:

$$\dot{W} = \int \bar{\sigma} \cdot \dot{\bar{\phi}} \cdot dV \qquad (1)$$

where $\dot{W}$ = total energy of deformation

V = volume worked underneath the roller

$\bar{\sigma}$ = effective stress

$\dot{\bar{\phi}}$ = effective strain rate

$\bar{\sigma}$ will be assumed to be a constant and $\dot{\bar{\phi}}$ is to be derived from the velocity field. V is the product of the contact area between the cone and the roller and the thickness of the cone. The angles and dimensions of the cone and the shape and dimensions of the roller are shown in Figs. 1 and 3 respectively.

Strain Rates

The strain rates in cylindrical polar coordinates assume the form:[3]

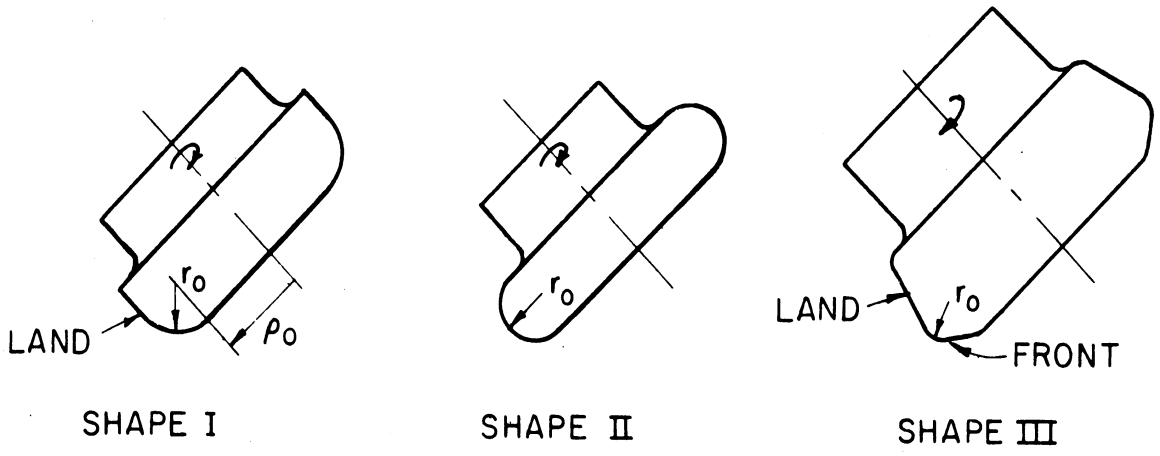

Figure 3. The Roller.

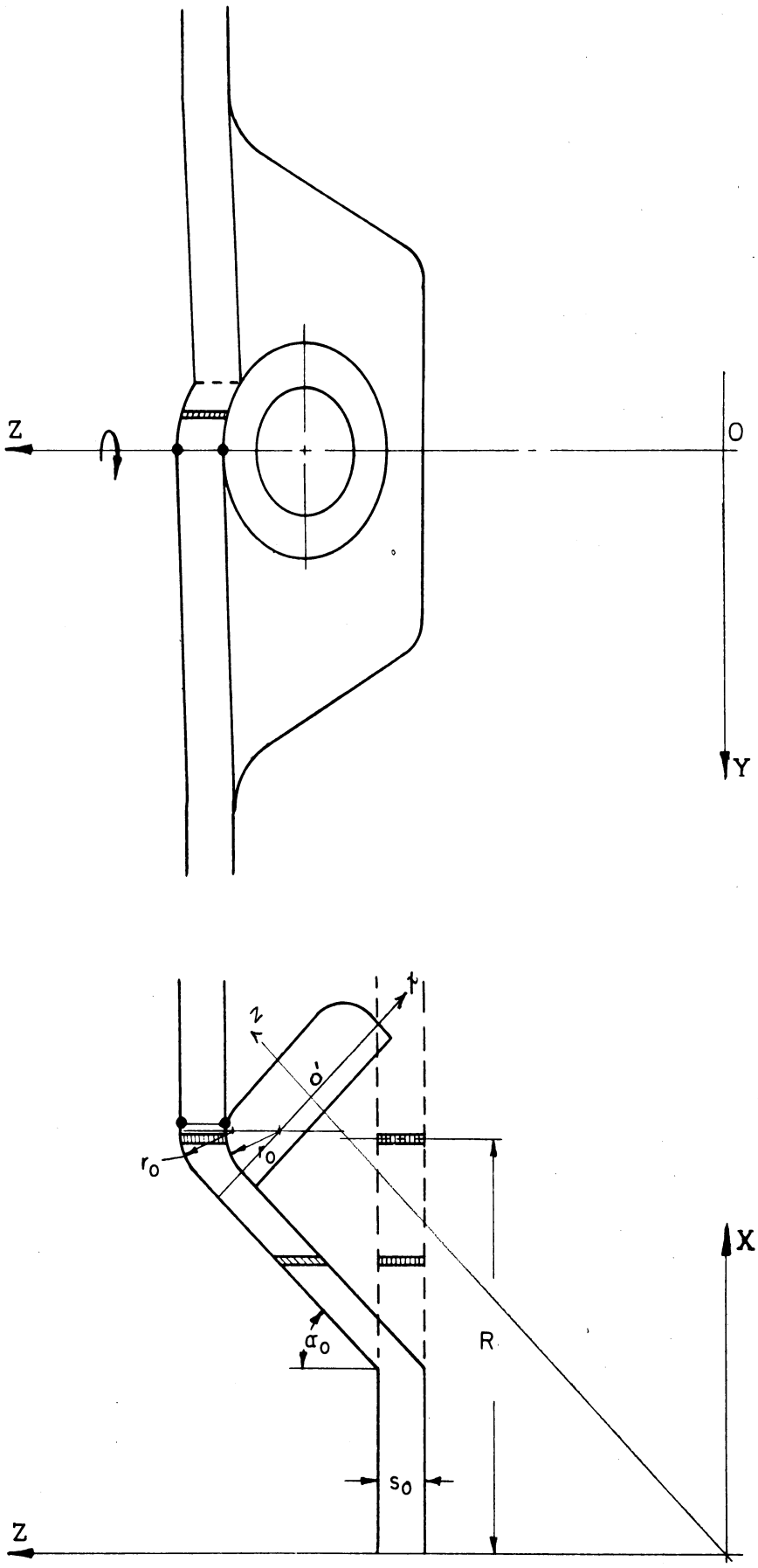

Figure 4. The Deformations.

$$\left.\begin{aligned}
&\dot{\varepsilon}_{RR} = \frac{\partial U_R}{\partial R};\quad \dot{\varepsilon}_{\theta\theta} = \frac{U_R}{R} + \frac{1}{R}\frac{\partial U_\theta}{\partial \theta};\quad \dot{\varepsilon}_{ZZ} = \frac{\partial U_Z}{\partial Z}\\
&\dot{\varepsilon}_{R\theta} = \frac{1}{2}\left(\frac{1}{R}\frac{\partial U_R}{\partial \theta} + \frac{\partial U_\theta}{\partial R} - \frac{U_\theta}{R}\right)\\
&\dot{\varepsilon}_{RZ} = \frac{1}{2}\left(\frac{\partial U_R}{\partial Z} + \frac{\partial U_Z}{\partial R}\right)\\
&\dot{\varepsilon}_{\theta Z} = \frac{1}{2}\left(\frac{\partial U_\theta}{\partial Z} + \frac{1}{R}\frac{\partial U_Z}{\partial \theta}\right)
\end{aligned}\right\} \qquad (2)$$

Where $\dot{\varepsilon}_{RR}$, $\dot{\varepsilon}_{\theta\theta}$, $\dot{\varepsilon}_{ZZ}$, $\dot{\varepsilon}_{R\theta}$, $\dot{\varepsilon}_{RZ}$, and $\dot{\varepsilon}_{\theta Z}$ are the components of the strain rate tensor field; U_R, U_θ, and U_Z are the components of the velocity vector field.

In order to solve our particular deformation field, the velocity field under the roller was computed first.

Because the angular velocity of the spinning cone is constant, one gets the circumferential velocity at any point on the cone as follows:

$$U_\theta = 2\pi RN \qquad (3)$$

Where U_θ is the circumferential velocity

R is the radius of the point considered and

N is the velocity of rotation, r.p.m.

Also, because there is no change in the radius R at any point on the cone during spinning, the radial velocity (U_R) will be:

$$U_R = 0 \qquad (4)$$

It is apparent that the cone under the area of contact during deformation takes the shape of the roller. Let the geometry of the roller be described as follows:

$$Z = H(R,\theta,n) \qquad (5)$$

Thus, $$dZ = \frac{\partial Z}{\partial R}\cdot dR + \frac{\partial Z}{\partial \theta}\cdot d\theta + \frac{\partial Z}{\partial n}\cdot dn \qquad (6)$$

and $$U_Z = \frac{dZ}{dT} = \frac{\partial Z}{\partial R}\frac{dR}{dT} + \frac{\partial Z}{\partial \theta}\cdot\frac{d\theta}{dT} + \frac{\partial Z}{\partial n}\cdot\frac{dn}{dT} \qquad (7)$$

Where T is the time passed from time $T = T_o$ to the instant

n is the number of revolutions passed from time $T = T_o$ to the instant, and

U_Z is the velocity component in Z direction.

One now continues to compute the derivatives with respect to time in the following:

$$n = N(T - T_o) \tag{8}$$

$$\frac{dn}{dT} = N \tag{9}$$

$$\frac{d\theta}{dT} = \frac{U_\theta}{R} = 2\pi N \tag{10}$$

$$\frac{dR}{dT} = U_R = 0 \tag{11}$$

Substituting the above derivatives into Equation (7) yields:

$$U_Z = \frac{\partial Z}{\partial \theta} \cdot 2\pi N + \frac{\partial Z}{\partial n} \cdot N = N \left[2\pi \frac{\partial Z}{\partial \theta} + \frac{\partial Z}{\partial n} \right] \tag{12}$$

Therefore the complete velocity field can be summarized as:

$$\left.\begin{aligned} U_R &= 0 \\ U_\theta &= 2\pi RN \\ U_Z &= N \left[2\pi \frac{\partial Z}{\partial \theta} + \frac{\partial Z}{\partial n} \right] \end{aligned}\right\} \tag{13}$$

where the velocity field is a function of R, and θ only, and the derivatives $\frac{\partial Z}{\partial \theta}$ and $\frac{\partial Z}{\partial n}$ are yet to be defined from the equation of the roller.

Inserting the values of U_R, U_θ and U_Z from Equation (13) into Equation (2) one gets the following strain rate field:

$$\left.\begin{aligned} \dot{\varepsilon}_{RZ} &= \frac{1}{2} \cdot \frac{\partial U_Z}{\partial R} \\ \dot{\varepsilon}_{\theta Z} &= \frac{1}{2R} \cdot \frac{\partial U_Z}{\partial \theta} \\ \text{all other } \dot{\varepsilon}_{ij} &= 0 \end{aligned}\right\} \tag{14}$$

Stress-Strain Relation

Levy-Mises stress-strain rate law of plasticity (incremental theory) was used, that is,

$$\dot{\varepsilon}_{ij} = \mu S_{ij} \tag{15}$$

where S_{ij} and $\dot{\varepsilon}_{ij}$ are stress deviator and strain-rate deviator tensors respectively; $\frac{1}{\mu}$ is a modulus of plasticity and a function of $\dot{\varepsilon}_{ij}$.

Owing to volume constancy in plastic region, the plastic strain rate deviator is equal to the plastic strain rate itself, because

$$\dot{e} = \frac{1}{3}\dot{e}_{ii} \quad , \tag{16}$$

where $\dot{e}$ = hydrostatic strain rate and

$$\dot{e}_{ii} = \dot{e}_{11} + \dot{e}_{22} + \dot{e}_{33} = 0 \tag{17}$$

Let a term "I" be defined as

$$I = \frac{1}{2}\left(\dot{\varepsilon}_{xx}^2 + \dot{\varepsilon}_{yy}^2 + \dot{\varepsilon}_{zz}^2\right) + \frac{1}{4}\left(\dot{\gamma}_{xy}^2 + \dot{\gamma}_{yz}^2 + \dot{\gamma}_{zx}^2\right) = \frac{1}{2}\dot{\varepsilon}_{ij}\,\dot{\varepsilon}_{ij} \text{ (tensor)} \tag{18}$$

It has been shown by Prager and Hodge[4] that:

$$S_{ij} = \frac{k\,\dot{\varepsilon}_{ij}}{\sqrt{\frac{1}{2}\,\dot{\varepsilon}_{kl}\cdot\dot{\varepsilon}_{kl}}} \tag{19}$$

Where k = yield limit in simple shear = $\frac{\sigma_o}{\sqrt{3}}$.

The stress deviator field can therefore be written as follows:

$$\left.\begin{aligned} S_{RZ} = \tau_{RZ} &= \frac{k\,\dot{\varepsilon}_{RZ}}{\sqrt{\dot{\varepsilon}_{RZ}^2 + \dot{\varepsilon}_{\theta Z}^2}} \\ \text{and}\quad S_{\theta Z} = \tau_{\theta Z} &= \frac{k\,\dot{\varepsilon}_{\theta Z}}{\sqrt{\dot{\varepsilon}_{RZ}^2 + \dot{\varepsilon}_{\theta Z}^2}} \\ \text{all other } S_{ij} &= 0. \end{aligned}\right\} \tag{20}$$

The Power

Let the rate of work per unit volume = $\dot{w}$

$$\dot{w} = \sigma_{ij}\cdot\dot{\varepsilon}_{ij} \tag{21}$$

Now $$\sigma_{ij} = S_{ij} + S\delta_{ij} \tag{22}$$

where S_{ij} = deviator stress

S = hydrostatic tensor

and δ_{ij} = unit tensor, equals 1 when i=j
equals 0 when i≠j

Again because of volume constancy, $\dot{\varepsilon}_{ii} = 0$, thus $\dot{w} = S_{ij}\,\dot{\varepsilon}_{ij}$ (23)

Therefore $\dot{w} = S_{ij}\cdot S_{ij}\sqrt{\frac{1}{2}\,\dot{\varepsilon}_{ij}\cdot\dot{\varepsilon}_{ij}}\cdot\left(\frac{1}{k}\right)$ (24)

Now that the yielding condition $J_2 = \frac{1}{2}\,S_{ij}S_{ij} = k^2$, (25)

One gets: $\dot{w} = 2k\sqrt{\frac{1}{2}\,\dot{\varepsilon}_{ij}\cdot\dot{\varepsilon}_{ij}} = \frac{2}{\sqrt{3}}\cdot\sigma_o\sqrt{\frac{1}{2}\,\dot{\varepsilon}_{ij}\cdot\dot{\varepsilon}_{ij}}$

$$= \frac{2}{\sqrt{3}}\,\sigma_o\sqrt{\dot{\varepsilon}_{RZ}^2 + \dot{\varepsilon}_{\theta Z}^2} = \frac{2}{\sqrt{3}}\,\sigma_o\sqrt{\left(\frac{1}{2}\,\frac{\partial U_Z}{\partial R}\right)^2 + \left(\frac{1}{2R}\,\frac{\partial U_Z}{\partial \theta}\right)^2}$$

$$= \frac{\sigma_o}{\sqrt{3}}\sqrt{\left(\frac{\partial U_Z}{\partial R}\right)^2 + \left(\frac{1}{R}\,\frac{\partial U_Z}{\partial \theta}\right)^2} \tag{26}$$

The rate of total work done on metal under the contact area, $\dot{W} = \int \dot{w} dV$, that is,

$$\dot{W} = \int_{vol.} \frac{\sigma_o}{\sqrt{3}} \sqrt{\left(\frac{\partial U_Z}{\partial R}\right)^2 + \left(\frac{1}{R}\frac{\partial U_Z}{\partial \theta}\right)^2} \cdot dV$$

$$= \frac{\sigma_o}{\sqrt{3}} \int_{\substack{surface \\ area}} \left[\int_{Z=0}^{Z=s_o} \sqrt{\left(\frac{\partial U_Z}{\partial R}\right)^2 + \left(\frac{1}{R}\cdot\frac{\partial U_Z}{\partial \theta}\right)^2} \cdot dZ \right] ds \qquad (27)$$

Where ds = infinitesimal surface area (ds = Rd θ dR).

Because the terms under the square root are independent of Z, one gets:

$$\dot{W} = \frac{\sigma_o}{\sqrt{3}} s_o \int_\theta \cdot \int_R \cdot R \sqrt{\left(\frac{\partial U_Z}{\partial R}\right)^2 + \left(\frac{1}{R}\frac{\partial U_Z}{\partial \theta}\right)^2} \, dR \, d\theta \qquad (28)$$

Where the integration is to be done along the boundaries of the area of contact between the roller and the cone.

Let $\dot{W}'$ be designated as weighted power, and defined as

$$\dot{W}' = \frac{\dot{W}\sqrt{3}}{\sigma_o s_o N} \qquad (29)$$

or

$$\dot{W}' = \frac{1}{N} \int_\theta \int_R R \sqrt{\left(\frac{\partial U_Z}{\partial R}\right)^2 + \left(\frac{1}{R}\frac{\partial U_Z}{\partial \theta}\right)^2} \, dR \, d\theta \qquad (30)$$

Also let

$$\delta = \left[\frac{1}{R}\frac{\partial U_Z}{\partial \theta} \Big/ \frac{\partial U_Z}{\partial R}\right]^2 \qquad (31)$$

The following equation yields

$$\dot{W}' = \frac{1}{N} \int_\theta \int_R R \sqrt{1+\delta} \left(\frac{\partial U_Z}{\partial R}\right) dR \, d\theta \qquad (32)$$

The function of the cylindrical portion of the roller is to smooth out the feed mark and the work done by it is very small compared with that done by the torus. Thereby the work done by the cylindrical portion of the roller is neglected. The actual and simplified areas of contact are shown in Figs. 5 and 6. Assuming $\hat{\delta}$ is independent of R and θ, one has:

$$\dot{W}' = \frac{1}{N} \sqrt{1+\hat{\delta}} \int_\theta \int_R R \left(\frac{\partial U_Z}{\partial R}\right) dR \, d\theta \qquad (33)$$

Since $\frac{\partial U_Z}{\partial R}$ changes appreciably for slight change of R, R itself can be considered as constant, ($R \doteq R_o$). Therefore,

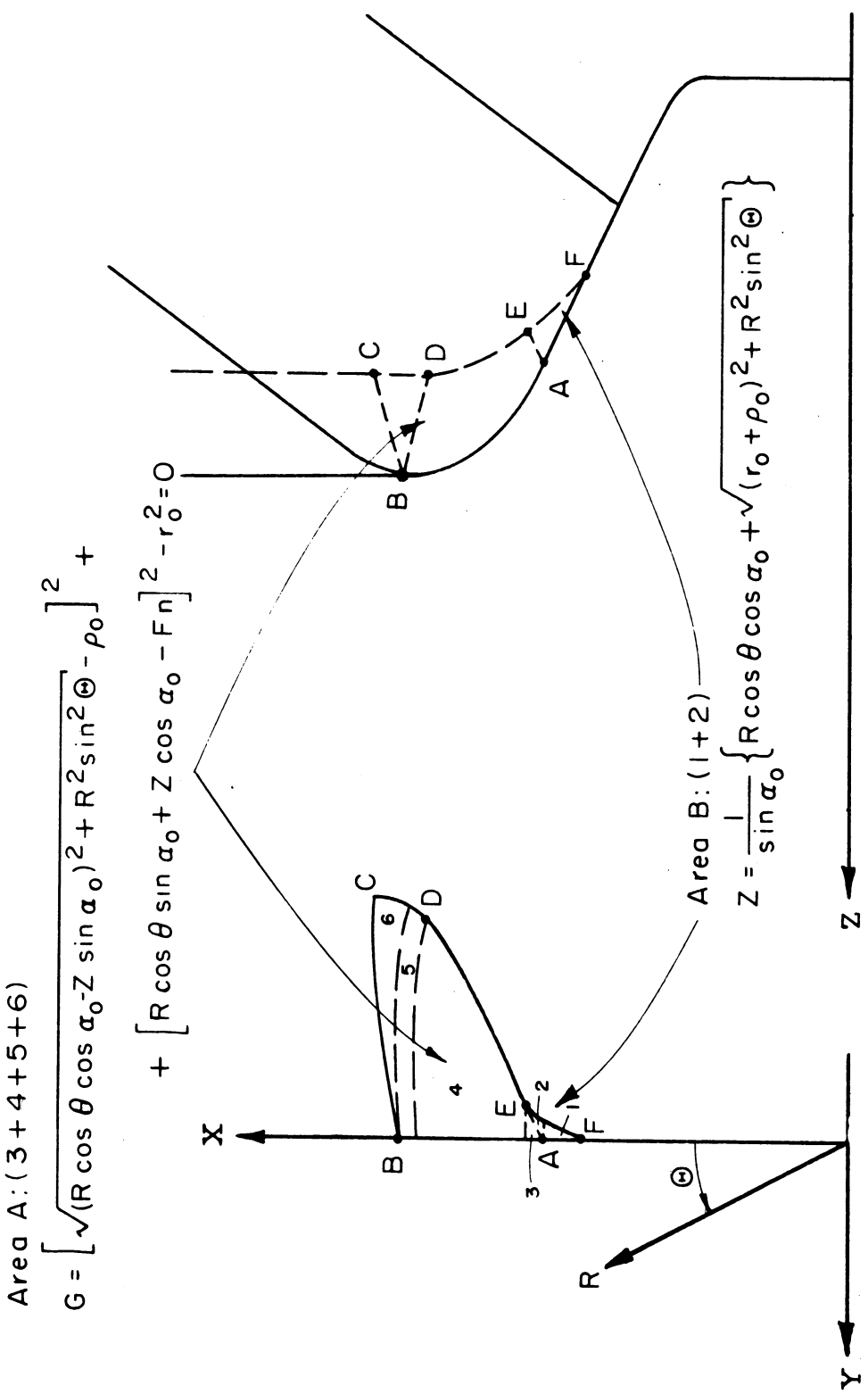

Figure 5. The Area of Contact.

$$\dot{W}' = \frac{\sqrt{1+\delta}}{N} R_o \int_\theta \left[|U_Z| \begin{array}{l} R = \text{upper limit} \\ R = \text{lower limit} \end{array} \right] d\theta = \frac{\sqrt{1+\delta}}{N} R_o \int_\theta \Delta U_Z \, d\theta \quad (34)$$

Again since $U_Z = N \left[2\pi \frac{\partial Z}{\partial \theta} + \frac{\partial Z}{\partial n} \right]$, one has

$$\dot{W}' = \sqrt{1+\delta} \cdot R_o \left\{ \int_\theta 2\pi \left(\Delta \frac{\partial Z}{\partial \theta} \right) d\theta + \int_\theta \left(\Delta \frac{\partial Z}{\partial n} \right) d\theta \right\} \quad (35)$$

Now that $\int_\theta \left(\Delta \frac{\partial Z}{\partial \theta} \right) d\theta = \Delta Z = F \cos\alpha_o$ (36)

$$\dot{W}' = 2\pi R_o \sqrt{1+\delta} \; F \cos\alpha_o + \sqrt{(1+\delta)} \, R_o \cdot \int_\theta \left(\Delta \frac{\partial Z}{\partial n} \right) d\theta \quad (37)$$

The value of $\frac{\partial Z}{\partial n}$ can be evaluated from the equation of a torus, the geometry of which can be approximated by the following equation (see Fig. 7):

$$(a - Z)^2 + (b - X)^2 = r_o^2 \quad (38)$$

From Fig. 7 also one has

$$Z = Fn \cos\alpha_o + \rho_o \sin\alpha_o + \sqrt{r_o^2 - \left[b - R \cdot \cos\theta \right]^2} \quad (39)$$

$$\frac{\partial Z}{\partial n} = F \cdot \cos\alpha_o + \frac{\left[R \cos\theta - \left(Fn \cdot \sin\alpha_o - \rho_o \cos\alpha_o \right) \right] \cdot F \cos\alpha_o}{\sqrt{r_o^2 - \left[R \cos\theta - \left(Fn \cdot \sin\alpha_o - \rho_o \cos\alpha_o \right) \right]^2}} \quad (40)$$

$$\Delta \frac{\partial Z}{\partial n} = \left(\frac{\partial Z}{\partial n} \right)_{R = \text{upper limit}} - \left(\frac{\partial Z}{\partial n} \right)_{R = \text{lower limit}} \quad (41)$$

Thus the equation W' can be evaluated except for the value of δ - the strain ratio, which will be dealt with in the following section.

Evaluation of the Strain Ratio

From the approximate equation of the torus, Equation (38), one can derive

$$\frac{U_Z}{N} = \frac{1}{N} \cdot \frac{dZ}{dT} = F \cdot \cos\alpha_o - \frac{\left[R \cos\theta - \left(Fn \cdot \sin\alpha_o - \rho_o \cos\alpha_o \right) \right] \cdot \left[-R \sin\theta \cdot 2\pi - F \sin\alpha_o \right]}{\sqrt{r_o^2 - \left[R \cos\theta - \left(Fn \sin\alpha_o - \rho_o \cos\alpha_o \right) \right]^2}} \quad (42)$$

$$\frac{1}{N} \frac{\partial U_Z}{\partial R} = \frac{1}{(\sqrt{\psi})^3} \cdot \left[r_o^2 \cdot \cos\theta \left(2\pi R \cdot \sin\theta + F \sin\alpha_o \right) + 2\pi \sin\theta \cdot \psi (R \cos\theta - \beta \right] \quad (43)$$

and $$\frac{1}{N} \cdot \frac{1}{R} \cdot \frac{\partial U_Z}{\partial \theta} = \frac{1}{(\sqrt{\psi})^3} \left[- r_o^2 \sin\theta \left\{ 2\pi R \cdot \sin\theta + F \sin\alpha_o \right\} + 2\pi \cos\theta \cdot (R \cos\theta - \beta) \cdot \psi \right] \quad (44)$$

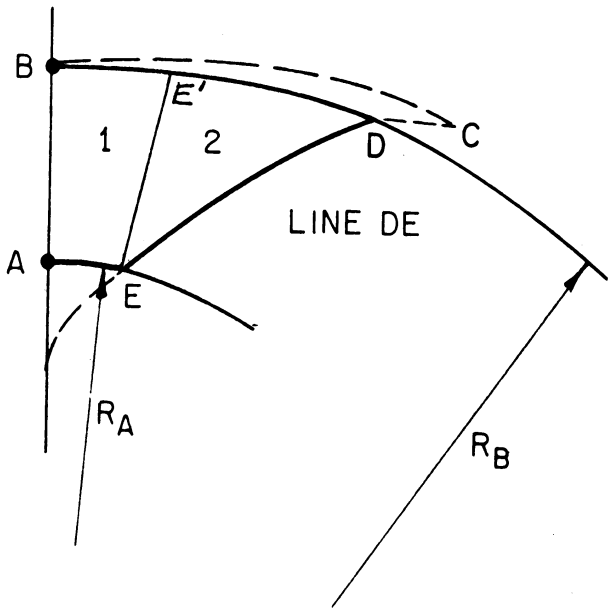

Figure 6. Approximated Area of Contact.

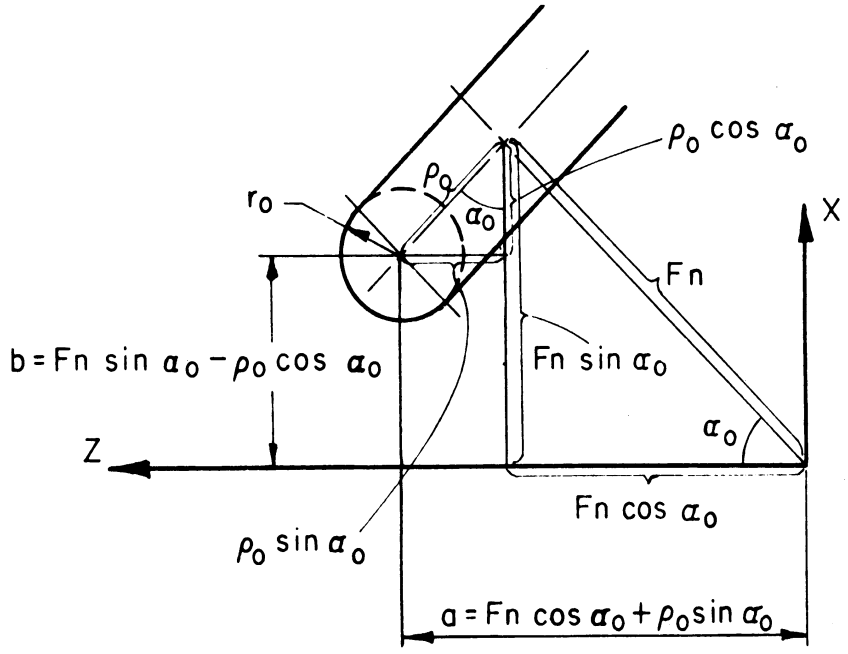

Figure 7. Approximating the Torus by a Cylinder.

Thus,

$$\delta = \left\{ \frac{\frac{1}{R}\frac{\partial U_Z}{\partial \theta}}{\frac{\partial U_Z}{\partial R}} \right\}^2 = \left\{ \frac{2\pi \cos\theta (R\cos\theta - \beta)\psi - r_o^2 \sin\theta\,(2\pi R \sin\theta + F\sin\alpha_o)}{2\pi \sin\theta\,(R\cos\theta - \beta)\psi + r_o^2 \cos\theta\,(2\pi R\sin\theta + F\sin\alpha_o)} \right\}^2 \quad (45)$$

where $\beta = Fn\cdot\sin\alpha_o - \rho_o\cos\alpha_o$, and

$$\psi = r_o^2 - \left[R\cos\theta - (Fn\cdot\sin\alpha_o - \rho_o\cos\alpha_o)\right]^2 \quad (46)$$

Evaluation of the Power

It now remains to evaluate numerically the spinning power from the following equation:

$$\dot{W}' = \sqrt{1+\delta}\left\{2\pi R_o F\cos\alpha_o + \int_\theta \left(\Delta\frac{\partial Z}{\partial n}\right) d\theta\right\} \quad (47)$$

where δ is defined in Equation (45).

Combining Equations (40) and (41), one has

$$\Delta\frac{\partial Z}{\partial n} = \frac{R_{upper}\cos\theta - \beta}{\sqrt{r_o^2 - \left(R_{upper}\cos\theta - \beta\right)^2}} - \frac{R_{lower}\cos\theta - \beta}{\sqrt{r_o^2 - \left(R_{lower}\cos\theta - \beta\right)^2}} \quad (48)$$

and, δ is solved as $\delta_{average}$ for the area of contact.

The boundaries of the approximated area of contact (Fig. 6) will now be computed. These boundaries are derived from the intersection of the cone with the roller.

The equation of the toric portion of the roller (see Appendix) is:

$$G = \left[\sqrt{(R\cos\theta\cos\alpha_o - Z\sin\alpha_o)^2 + R^2\sin^2\theta} - \rho_o\right]^2 + \left[R\cos\theta\sin\alpha_o + Z\cos\alpha_o - Fn\right]^2 - r_o^2 = 0 \quad (49)$$

and the equation of the portion of the cone which is in the process of being deformed (zone 2 of Fig. 8) is:

$$Z = b + \sqrt{b^2 - c}$$

where

$$b = \rho_o\sin\alpha_o + F\left(n - \frac{\theta}{2\pi}\right)\cos\alpha_o \doteq \rho_o\sin\alpha_o + F(n-1)\cos\alpha_o$$

$$c = (R\cos\alpha_o + \rho_o)^2 + \left[R\sin\alpha_o - F\left(n - \frac{\theta}{2\pi}\right)\right]^2 - r_o^2 \doteq (R\cos\alpha_o + \rho_o)^2 + \left[R\sin\alpha_o - F(n-1)\right]^2 - r_o^2 \quad (50)$$

Area of Contact

The area of contact between the roller and the cone is shown in Fig. 5 and an approximated one is shown in Fig. 6. The boundaries of the approximate area of contact can now be described line by line as follows:

Line AB

$$\begin{cases} (R\cos\alpha_0 - Z\sin\alpha_0 + \rho_0)^2 + (R\sin\alpha_0 + Z\cos\alpha_0 - Fn)^2 - r_0^2 = 0 \\ \theta = 0 \end{cases} \tag{51}$$

Line BD

$$R = R_B = F\left(n - \frac{\theta}{2\pi}\right)\sin\alpha_0 - \rho_0\cos\alpha_0 \doteq F(n-1)\cdot\sin\alpha_0 - \rho_0\cos\alpha_0 \tag{52}$$

Line DE

Line DE is computed from the intersection of the roller, G = 0, with zone 2 of the cone. G and zone 2 of the cone were defined previously by Equations (49) and (50) respectively.

Line AE

$$R = R_A = R_0 = F\left(n - \frac{\theta}{2\pi}\right)\sin\alpha_0 - (\rho_0 + r_0)\cos\alpha_0 \doteq F(n-1)\cdot\sin\alpha_0 - (\rho_0 + r_0)\cos\alpha_0 \tag{53}$$

Line EE'

$\theta = \theta_E$ and θ_E is found from the equation of the line DE for the value of $R = R_A$.

The boundary line DE as well as the values of θ_E and δ were computed on the IBM 650 digital computer. The numerical method used is described in Avitzur's thesis[5]. The actual boundaries of the area of contact (Fig. 5) are fully defined in the same reference.

In order to calculate the total energy of deformation under the torus, it is necessary to integrate within the boundaries of R and θ. Since the boundaries of integration have to be solved numerically, the IBM 650 digital computer was also used for the numerical evaluation of the integrals. Even though a computer was used, it is necessary to simplify the boundaries as shown by the dotted lines in Fig. 6. The programming of the computer is not shown in the paper for obvious reasons.

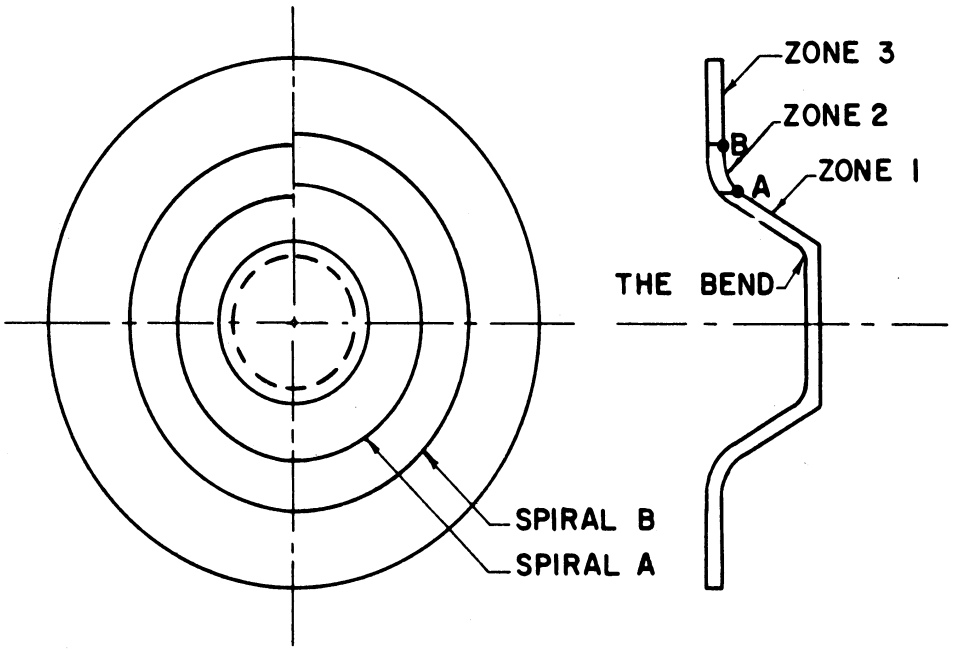

Figure 8. Zones of the Cone.

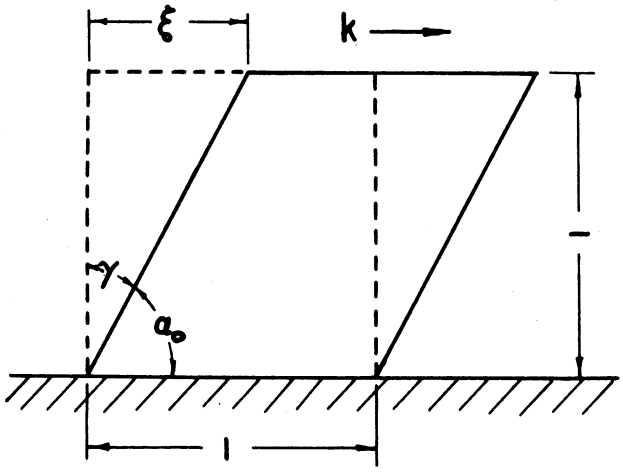

Figure 9. Deformation of a Cube by Pure Shear.

Forces

The total spinning power can be divided into the feed power and the tangential power, $\dot{W}_F$ and $\dot{W}_T$ respectively. Since $\dot{W}_F$ is small compared with $\dot{W}_T$ as observed from the experiment, the former is neglected here. Thus

$$\dot{W}_T = t \cdot U_\theta \tag{54}$$

where t = tangential force.

Numerical calculations of the tangential forces versus feed, included angle and round-off radius were plotted and shown in Figs.13, 14, and 15, respectively.

Solving the Power by a Simplified but Approximate Method (Deformation Theory)

It is seemingly difficult to calculate the spinning power and the tangential force. What is more, the necessity of using a digital computer to evaluate the integrals handicaps one in getting a quick numerical answer. Therefore, the following simple method is suggested to obtain an approximate power and tangential force with comparatively little effort.

A cubic block of unit volume as shown in Fig. 9 is subjected to pure shear with load, $k \frac{\text{lb.}}{\text{sq.in.}} \times 1$ sq. in. = k lbs.,

shear strain = γ

displacement $\xi = 1 \cdot \tan\gamma$

work per unit volume = $w = \frac{\sigma_0}{\sqrt{3}} \tan\gamma$ (55)

total volume worked on the cone = $V = 2\pi RN\, s_0\, F \cdot \sin\alpha_0 \frac{\text{in}^3}{\text{min}}$ (56)

and $\gamma = 90^0 - \alpha_0$ (57)

$\dot{W}$ = total power = $2\pi RN \sin\alpha_0\, s_0\, F \frac{\sigma_0}{\sqrt{3}} \tan\gamma = \frac{2}{\sqrt{3}}\pi\sigma_0\, s_0 NFR \cos\alpha_0$ (58)

Numerical calculations for a few examples of the tangential forces using this simplified method were also plotted in Figs. 13, 14 and 15 in dotted lines.

EXPERIMENTS AND RESULTS

Two types of experiments were conducted. One was designed to study the nature of the deformation in spinning. The other was designed to measure forces between the tool and the work, and also the spinning power.

1. Investigation of the Deformation Pattern

In the original disk .0125 inch holes were drilled and plugged with "sculp" metal (al. alloy) as shown in Fig. 10. After the cones were spun, the metal was carefully cut and filed until the holes were revealed. From the direction of the plugs, a three-dimensional deformation picture was constructed. A typical picture of the holes is shown in Fig. 11. This cone was spun and checked by the Cincinnati Milling Machine Company as part of a study conducted there. Detailed comparisons between the model cone and actual cones is given in Ref. 5.

In Fig. 12 a top view or the radial line of holes shows the shear $\varepsilon_{R\theta}$ of the cone. The angle α_θ indicates the extent to which the outer surface slipped over the inner surface of the cone. Numerical measurements of the distortion of the plugged holes can be found in Ref. 5.

In the analytical approach it was assumed that $\alpha_\theta = \alpha_R = 0$. It was observed experimentally that α_θ and α_R do not exceed a few degrees. In standard practice α_o is not over 75^o, which means that the minimum shear angle (γ) is over 15^o. Since α_θ and α_R are much smaller than 15^o, it is justified to assume that $\alpha_R = \alpha_\theta = 0$.

In the analytical approach ε_{RZ} was further assumed as pure shear, which means that $\alpha = 0$. This assumption does not actually hold. For large α_o, it seems that the deformation is closer to pure bending. For smaller α_o, the deformation is closer to pure shear rather than bending. For simplicity of the computation pure shear has been assumed throughout the study. (For the difference in power consumption between pure shear and bending, see Appendix 2 of Ref. 5.)

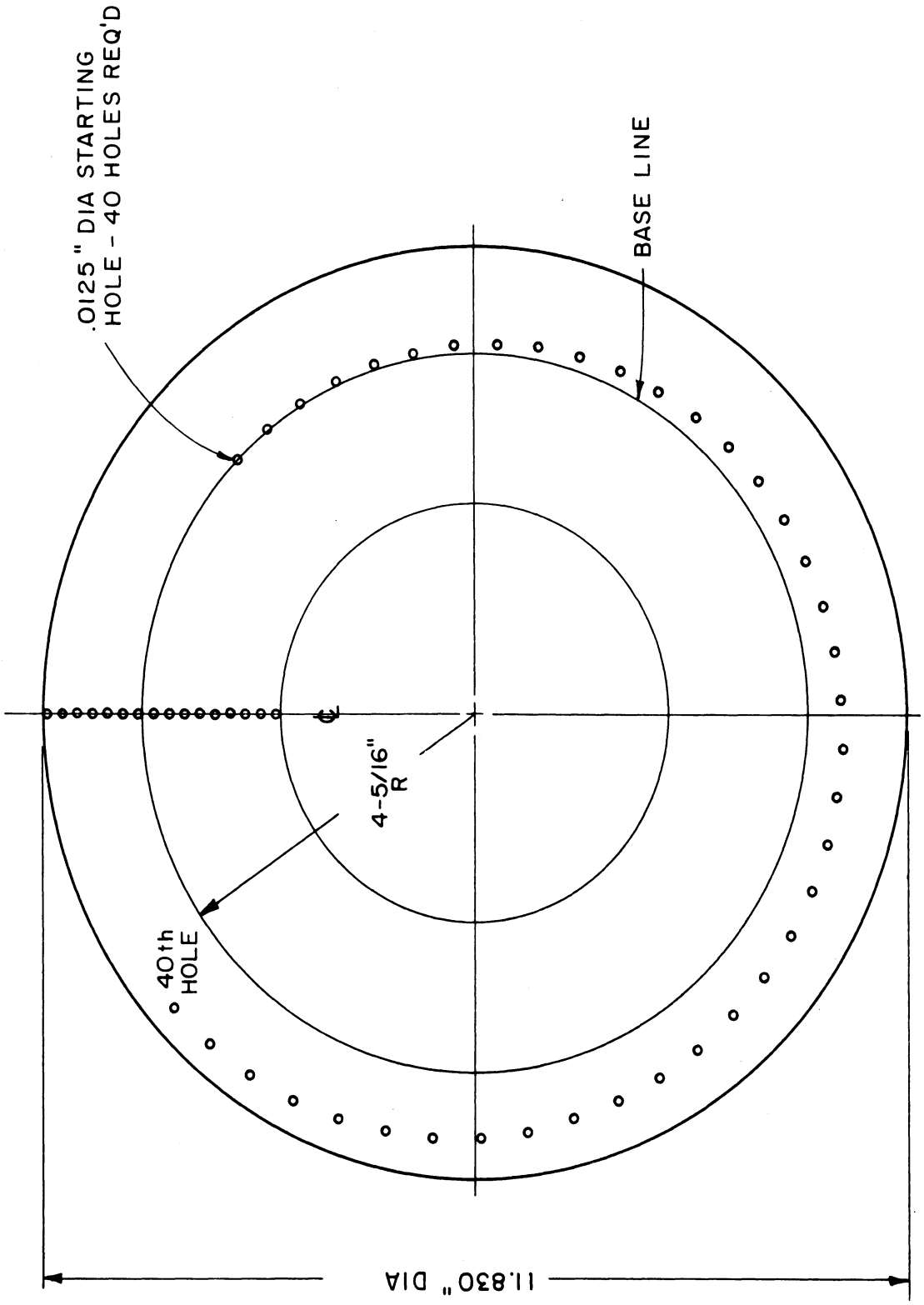

Figure 10. Holes in the Original Disc.

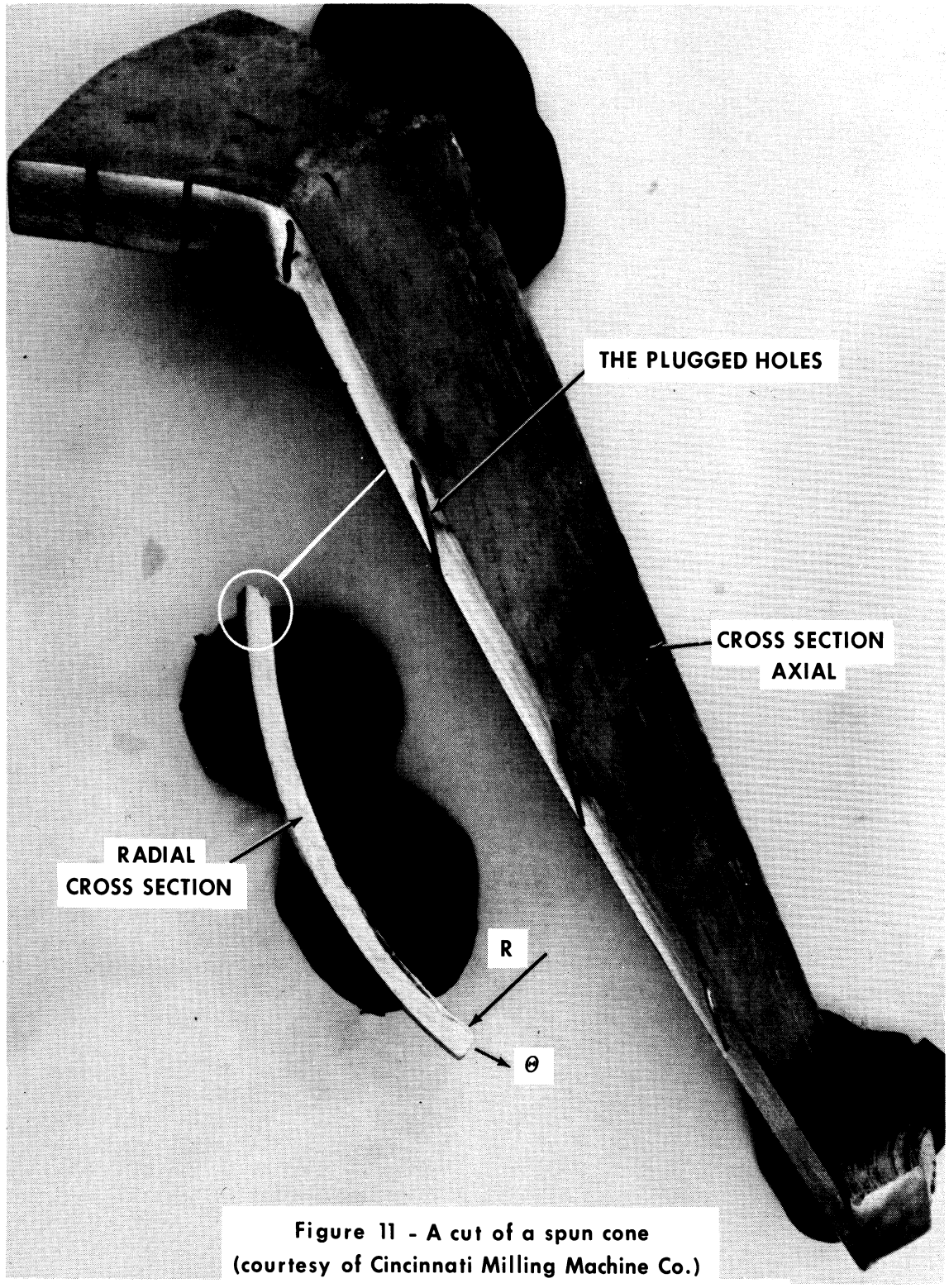

Figure 11 - A cut of a spun cone
(courtesy of Cincinnati Milling Machine Co.)

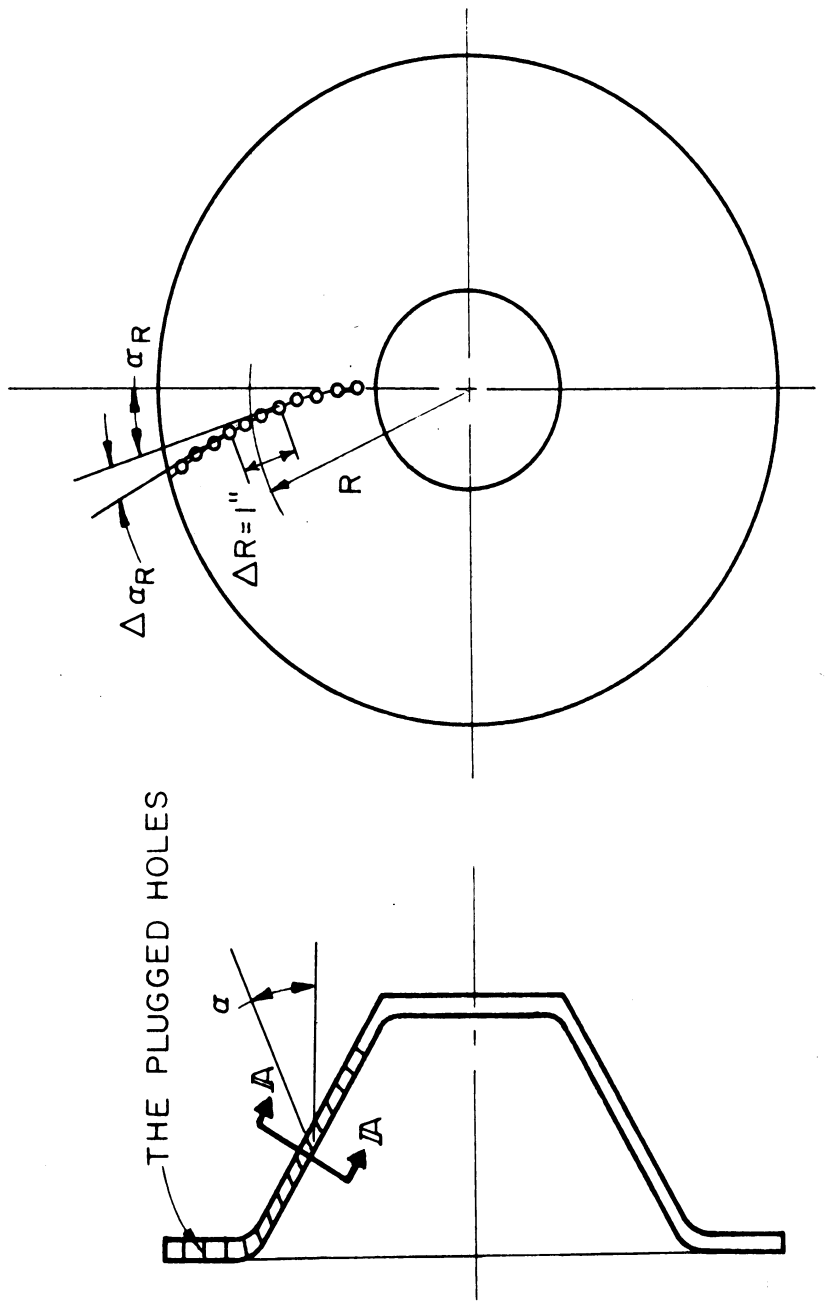

Figure 12. Directions of Holes in the Cone.

2. Measuring the Tangential Force and the Power

Two sets of experiments were conducted separately at the Cincinnati Milling Machine Company and Spincraft, Inc. In the Cincinnati Milling Machine Company tests were made to measure the forces. On their power spinning machine the roller is mounted on a three-dimensional dynamometer to measure the forces between the roller and the cone, the feed force, tangential force and the axial thrust. In this study only the tangential force is of interest to us. The experimental results are given in Table 1. The effect of the parameters, feed, included angle and the round-off radius on the tangential force was plotted and shown in Figs. 13, 14, and 15. In Spincraft, Inc. the power consumption of a d-c motor which drives the main spindle was measured. The set-up is shown in Fig. 16. The tare horsepower and the horsepower for spinning were separately measured. The power consumption for deforming the cone (W^o) is calculated as follows:

$$\dot{W}^o = \frac{\text{H.P. with load - tare H. P.}}{\text{efficiency}}$$

Since it is not easy to get the efficiency, it was assumed to be 100% for the first approximation. The experimental results are given in Table 2 and plots shown in Figs. 13, 14, and 15. The true stress and strain curve for aluminun 1100 - H was obtained and shown in Fig. 17. The yield strength is taken as an average of the true stresses in the region after yielding.

CONCLUSION

Results from theoretical analysis and experimental tests agree fairly well regardless of difficulties involved in the force and power measurement. The forces calculated from the simplified deformation theory is the lowest among all the forces computed from the lengthy analysis using incremental theory.

The effect of the variables on the tangential forces is observed as follows:

1. As the radius R_0 gets bigger, the tangential force is decreased, but it will never get to a value less than that predicted by the simplified method as shown in Figs. 13, 14, and 15.
2. The tangential force is linearly proportional to the yield limit σ_0, and the blank thickness s_0.
3. Increasing the feed (F) will increase the tangential force.
4. The larger the included angle ($2\alpha_0$) of the cone, the smaller will be the force.
5. As the roller round-off radius r_0 approaches zero, the efficiency approaches its best value (i.e., smallest force). As r_0 gets bigger than about 1/4 inch in practical conditions, a further increase of r_0 does not affect the force appreciably.
6. As the roller radius ρ_0 approaches zero, the force is least. When ρ_0 ranges between 6" and 10" ($6" \leq \rho_0 \leq 10"$), the tangential force changes very little.

TABLE 1

Cincinnati Results of Recorded Forces

1	2	3	4	5	6	7	8	9	10	11	12	13	14	15	16	17	18	19	20	21	22	23	24	25	26	27	28	29	30	31	32
									Speed						Cones Radius		Voltage Drawn		Excess Current Drawn		Power Consumed		Experimental Tangential Force				Experimental Weighted Tangential Force				
	Run Number	Material	Original Thickness	Half Included Angle	Feed per Revolution	Rollers "Round Off"	Rollers Radius	Yield Limit of Worked Cone	Initial	Halfway	Final	Representative	Feed per Minute		Small	Large	At Small Radius	At Large Radius	At Small Radius	At Large Radius	At Small Radius	At Large Radius	At Small Radius	At Large Radius	Weighting Factor		At Small Radius	At Large Radius			
			in.	°	ipr	inch		psi	rpm				ipm		inch		volts		amp		lb-in./min		lb		ppi		inch				
			S_o	α_o	F	r_o	ρ_o	σ_o	N_S	N_H	N_F	N	NF		R_1	R_2	V_1	V_2	ΔI_1	ΔI_2	$\dot{W}_1$	$\dot{W}_2$	t_1	t_2			t_1'	t_2'			
																					$\dot{W} = 531.V.\Delta I$		$t = \frac{\dot{W}}{2\pi RN}$		$\sigma_o \cdot S_o$		$t' = \frac{t}{\sigma_o \cdot S_o}$				
	M14	1100 Al	.250	35	.021	1/4	7	25000				300	6.3		1.0								75		6250			.012			
	M2	1100 Al	.250	35	.022	1/4	7	25000				300			1.0								50		6250			.008			
	M1	1100 Al	.250	35	.024	1/4	7	25000				300			1.0								95		6250			.015			
	M10	1100 Al	.250	35	.028	1/4	7	25000				300			1.0								100		6250			.016			
	M11	1100 Al	.250	35	.030	1/4	7	25000				300			1.0								120		6250			.019			
	M3	1100 Al	.250	35	.042	1/4	7	25000				300			1.0								130		6250			.021			
	M4	1100 Al	.250	35	.025	1/8	7	25000				300			1.0								155		6250			.025			
	M9	1100 Al	.250	35	.030	1/8	7	25000				300			1.0								120		6250			.019			
	M5	1100 Al	.250	35	.030	1/2	7	25000				300			1.0								105		6250			.017			
	D301	1100 Al	.375	35	.025	1/4	7	25000				300			1.0								200		9370			.021			
	D421	1100 Al	.485	35	.033	1/4	7	25000				300			1.0								300		12000			.025			
	M8	1100 Al	.250	21	.028	1/4	7	25000				300			1.0								130		6250			.021			
	M7	1100 Al	.250	21	.033	1/4	7	25000				300			1.0								105		6250			.017			
	M12	1100 Al	.250	21	.035	1/4	7	25000				300			1.0								115		6250			.0185			

TABLE 2

Spincraft Results of Recorded Power

1	2	3	4	5	6	7	8	9	10	11	12	13	14	15	16	17	18	19	20	21	22	23	24	25	26	27	28	29	30	31	32
	Run Number	Material	Original Thickness	Half Included Angle	Feed per Revolution	Rollers "Round Off"	Rollers Radius	Yield Limit of Worked Cone	Speed				Feed per Minute		Cones Radius		Voltage Drawn		Excess Current Drawn		Power Consumed		Experimental Tangential Force		Weighting Factor		Experimental Weighted Tangential Force				
									Initial	Halfway	Final	Representative			Small	Large	At Small Radius	At Large Radius	At Small Radius	At Large Radius	At Small Radius	At Large Radius	At Small Radius	At Large Radius			At Small Radius	At Large Radius			
			in.	°	ipr	inch		psi	rpm				ipm		inch		volts		amp		lb-in./min		lb		ppi		inch				
			S_o	α_o	F	r_o	ρ_o	σ_o	N_S	N_H	N_F	N	NF		P_1	R_2	V_1	V_2	ΔI_1	ΔI_2	$\dot{W}_1$	$\dot{W}_2$	t_1	t_2			t_1'	t_2'			
																					$\dot{W} = 531 \cdot V \cdot \Delta I$		$t = \frac{\dot{W}}{2\pi RN}$		$\sigma_o \cdot S_o$		$t' = \frac{t}{\sigma_o \cdot S_o}$				
	112	— Aluminum 1100-2S-O —	.081	27.5	.040	3/8	4 3/32	17,000	439	439	439				2 9/32	7.4	232	232	2	4.25	$247 \cdot 10^3$	$555 \cdot 10^3$	34.4	27.2	1380		.0250	.0197			
	113		.081	27.5	.060	3/8	4 7/32	17,000	440	439	435				2 9/32	7.4	232	232	3.3	7	$407 \cdot 10^3$	$860 \cdot 10^3$	56.7	42.5	1380		.0410	.0340			
	114		.081	27.5	.080	3/8	4 7/32	17,000	440	435	430				2 9/32	7.4	230	228	4.5	9.5	$550 \cdot 10^3$	$1150 \cdot 10^3$	76.5	57.5	1380		.0555	.0416			
	115		.081	27.5	.100	3/8	4 7/32	17,000	440	430	410				2 9/32	7.4	240	236	5	12	$638 \cdot 10^3$	$1500 \cdot 10^3$	89.0	78.5	1380		.0645	.0570			
	122		.077	54	.040	3/8	4 7/32	17,000	440	438	432				2 3/8	7 3/4	240	240	1	3	$127.5 \cdot 10^3$	$383 \cdot 10^3$	19.4	18.3	1310		.0148	.0140			
	124		.076	54	.080	3/8	4 7/32	17,000	438	435	432				2 3/8	7 3/4	236	236	2	6	$250 \cdot 10^3$	$750 \cdot 10^3$	38.2	35.8	1290		.0296	.0277			
	125		.076	54	.100	3/8	4 7/32	17,000	438	430	428				2 3/8	7 3/4	236	236	2.5	7.5	$316 \cdot 10^3$	$940 \cdot 10^3$	48.2	45.0	1290		.0374	.0350			
	132		.080	42.5	.040	3/8	4 7/32	17,000	440	438	438				3 5/8	8	236	236	X	4	—	$500 \cdot 10^3$	—	22.7	1360		—	.0167			
	133		.079	42.5	.060	3/8	4 7/32	17,000	440	438	434				3 5/8	8	236	234	3.5	6	$439 \cdot 10^3$	$747 \cdot 10^3$	44.0	34.2	1340		.0328	.0255			
	134		.079	42.5	.080	3/8	4 7/32	17,000	440	435	430				3 5/8	8	234	232	5	8	$620 \cdot 10^3$	$986 \cdot 10^3$	62.0	45.8	1340		.0462	.0342			
	135		.079	42.5	.100	3/8	4 7/32	17,000	440	435	429				3 5/8	8	234	232	5.5	11.5	$685 \cdot 10^3$	$1420 \cdot 10^3$	68.5	65.5	1340		.0510	.0490			
	45		.079	42.5	.080	1/8	4 1/2	17,000	440	435	430				3 5/8	8	236	236	4	8	$503 \cdot 10^3$	$1000 \cdot 10^3$	50.3	46.2	1340		.0375	.0345			
	148		.0805	42.5	.080	3/16	4 1/2	17,000	440	430	430				3 5/8	8	243	243	4.5	9	$580 \cdot 10^3$	$1160 \cdot 10^3$	57.7	53.6	1370		.042	.0390			

The Effect of the Feed (F) on the Weighted Tangential Force (t')

- - - Predicted by the Simplified Method (Deformation Theory)
——— Predicted by the Analysis (Incremental Theory)

The Tangential Force $t = \sigma_o \cdot s_o \cdot t'$ (lb.)
The Power $W = 2\pi R_o N t = 2\pi \cdot \sigma_o \cdot s_o \cdot R_o \cdot N \cdot t' \left(\frac{\text{lb.in.}}{\text{min.}}\right)$

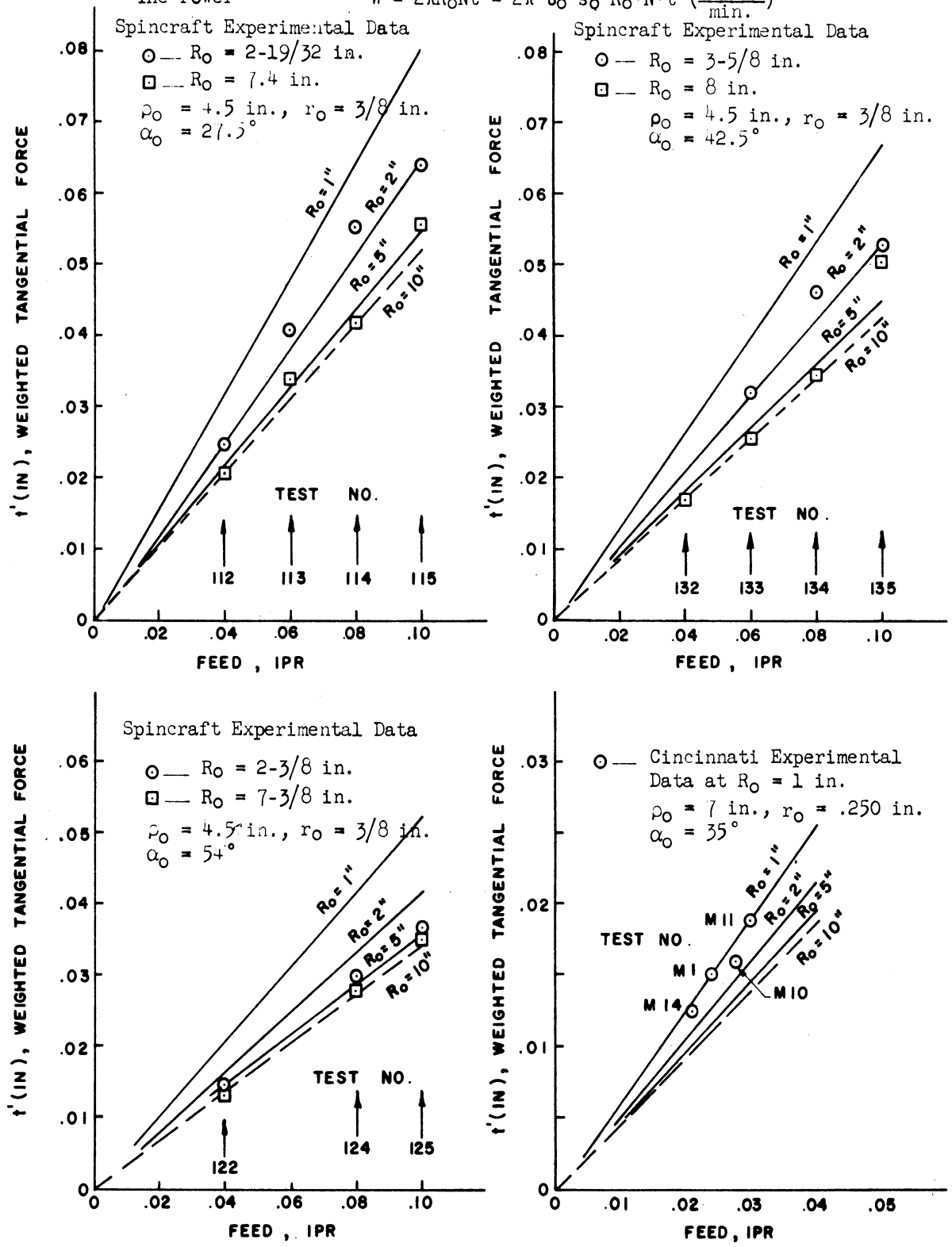

Figure 13. Curves of Tangential Forces Versus Feeds.

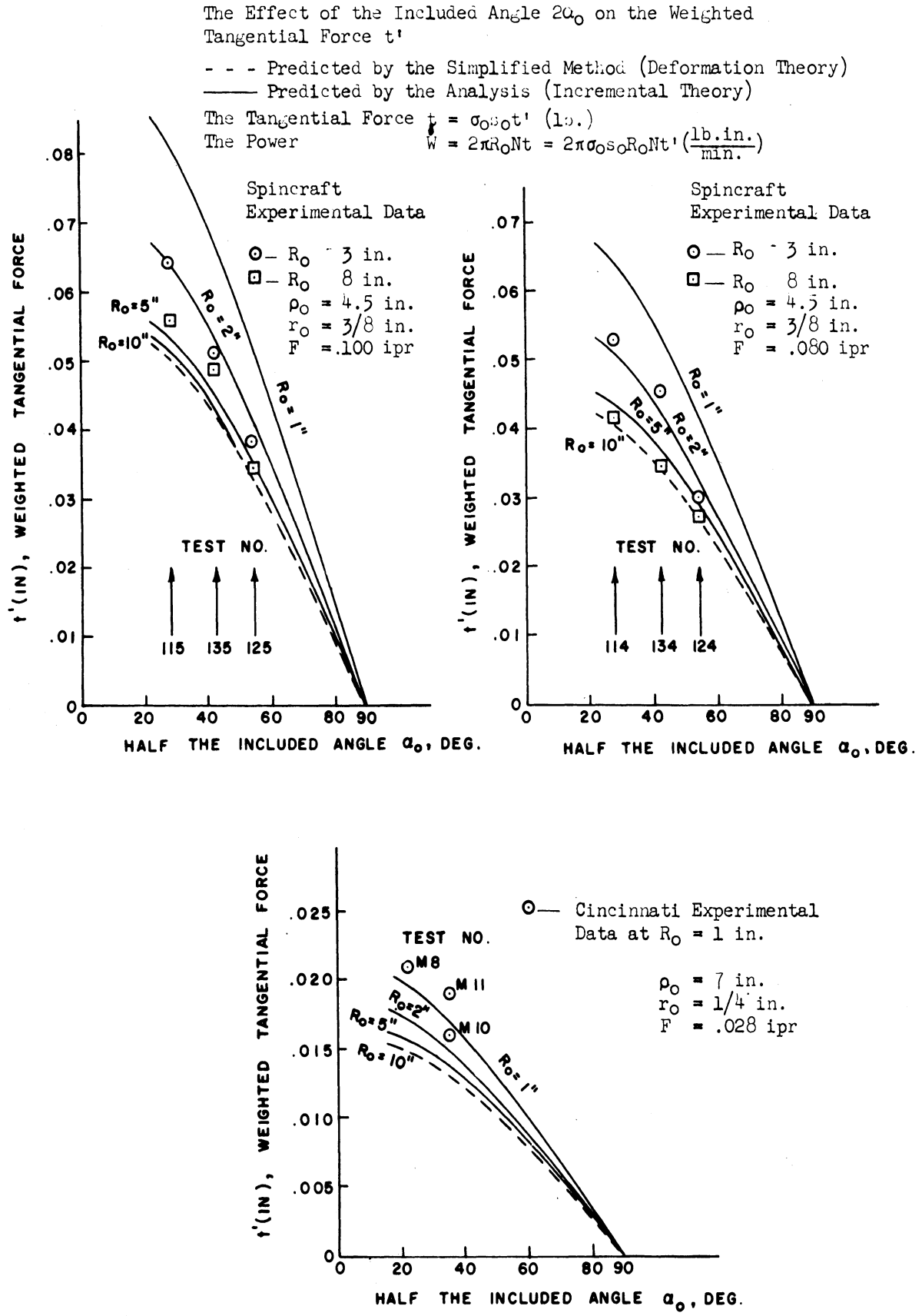

Figure 14. Curves of Tangential Forces Versus Included Angles of Cones.

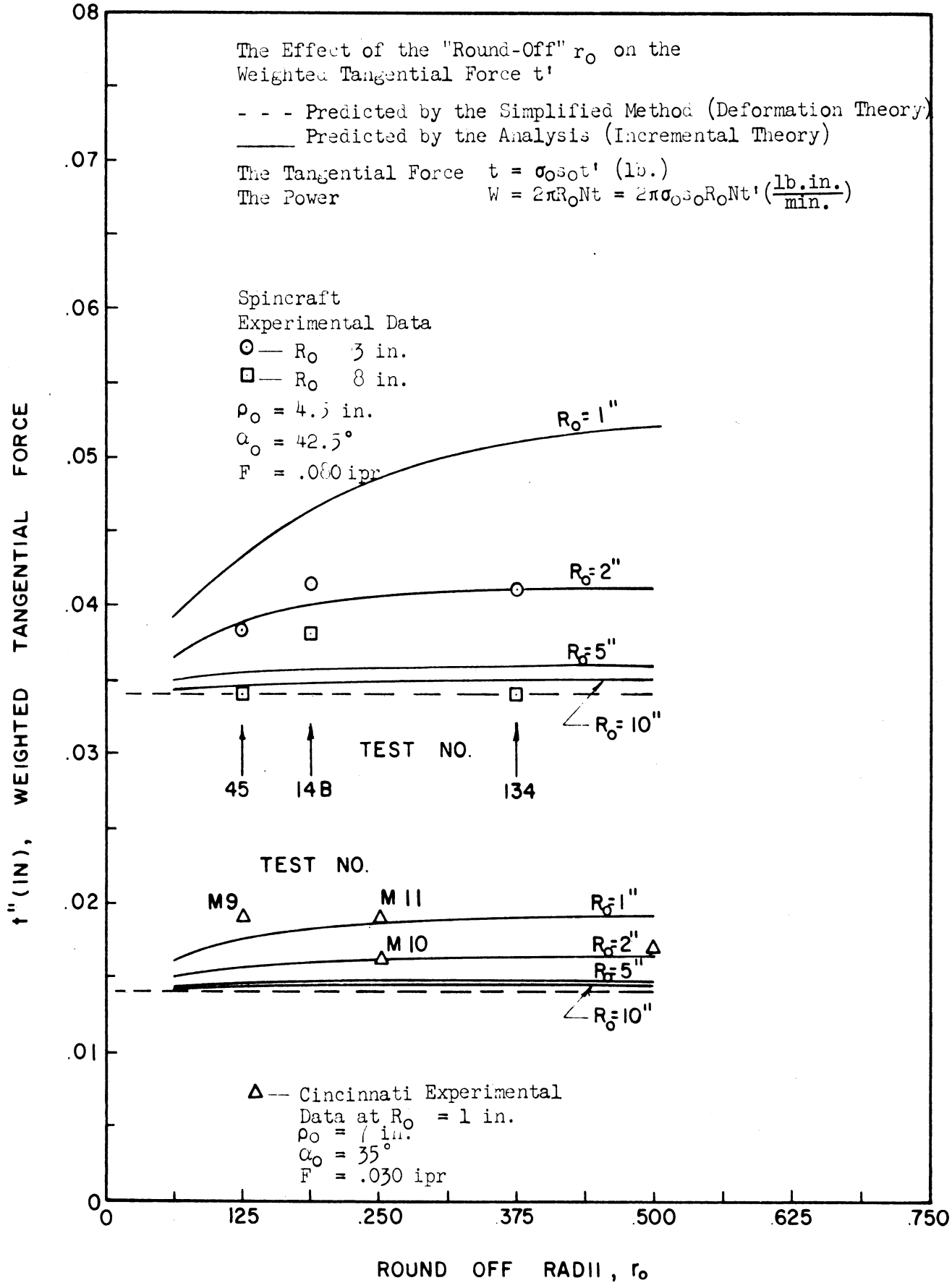

Figure 15. Curves of Tangential Forces Versus Round-Off Radii.

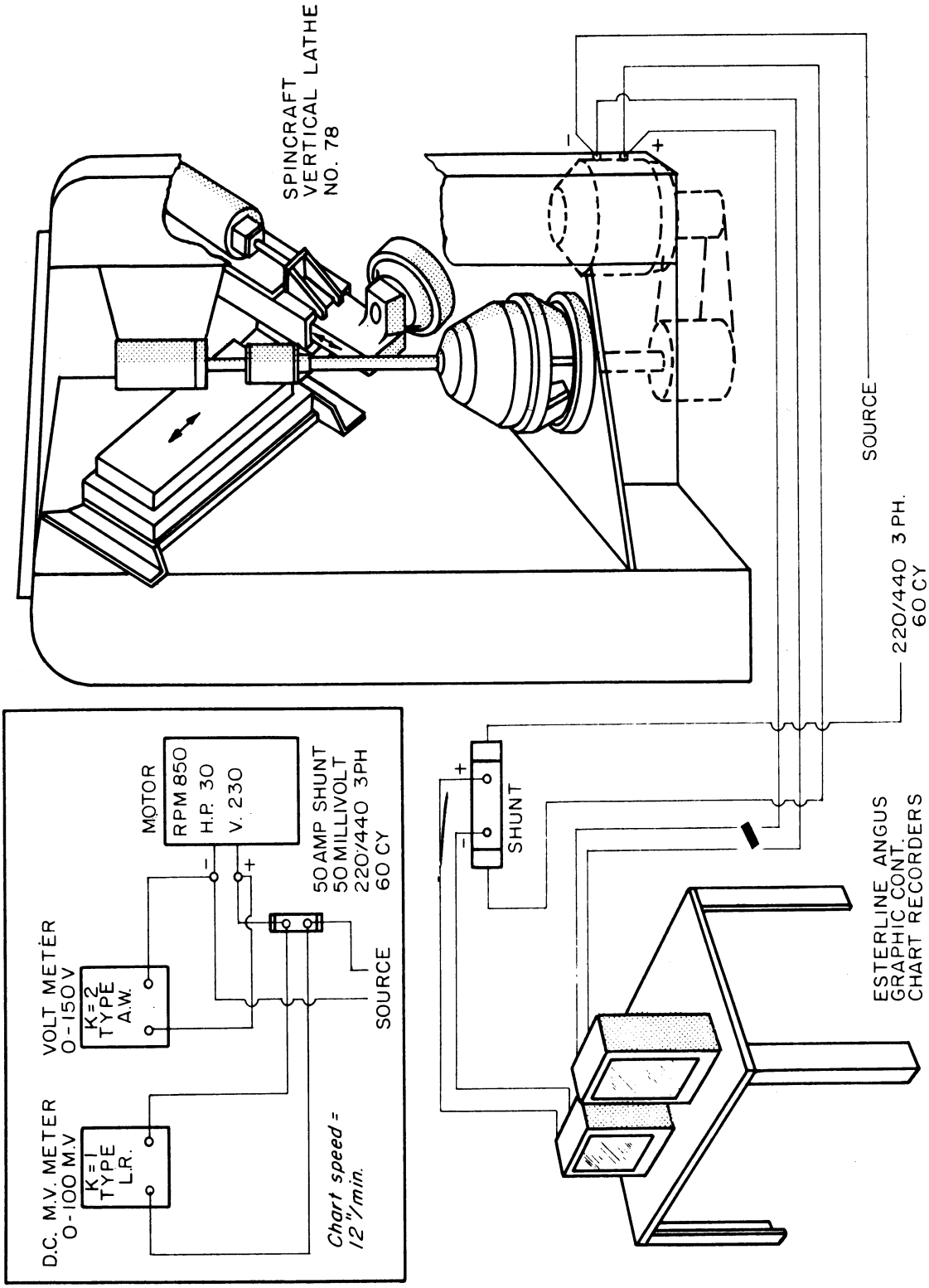

Figure 16. Spincraft Experimental Set Up. (Courtesy of Spincraft Inc.)

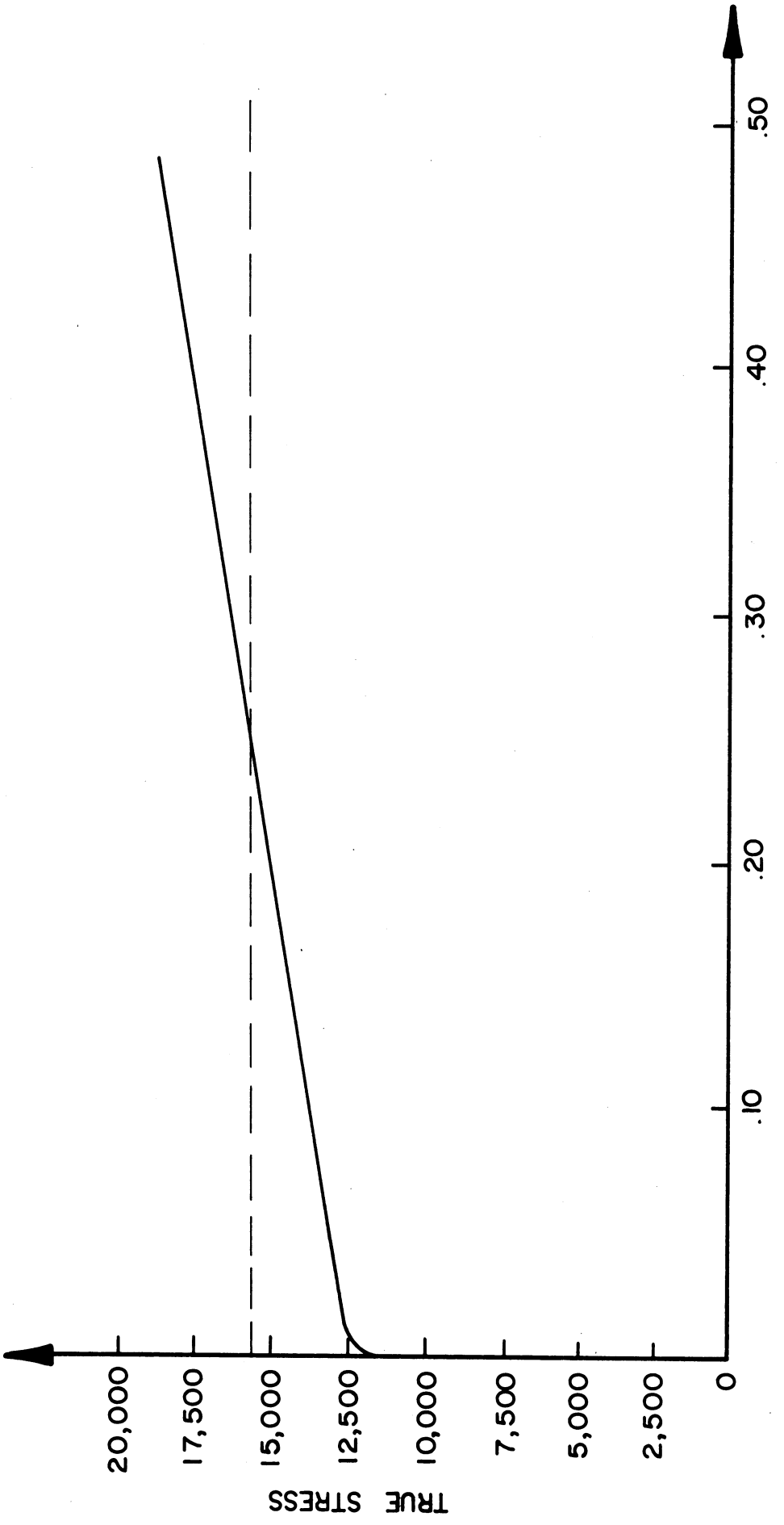

Figure 17. True Stress - True Strain for Al. 1100 (2S)H.

REFERENCES

1. a. Colding, B. N., Shear Spinning,ASME Paper No. 59-PROD-2, 1959.

   b. Feola, J. N., Experimental Analysis of Shear Deformation, M. S. Thesis, Syracuse University, January, 1955.

   c. Siebel, E., and Droge, K. A., "Forces and Material Flow in Spinning," Werkstattstechnik and Maschinenbau 45, No. 1, 6-9 (January, 1955).

2. Reichel, H., "Roll Spinning of Cone Shaped Aluminum Parts," Fertigungstechnik, 8, Part 1, No. 5, 181-184 (April, 1958); Part 2, No. 6, 252-260 (June, 1958).

3. Rouse, H. (Editor), Advanced Mechanics of Fluids, John Wiley and Sons, New York , 1959, p. 204.

4. Prager, W. and Hodge, P. H., Jr., Theory of Perfectly Plastic Solids, John Wiley and Sons, New York, 1951, p. 31.

5. Avitzur, B., Analysis of Power Spinning of Cones, Ph.D. Thesis, University of Michigan, June, 1959.

APPENDIX

TRANSFORMATION OF THE COORDINATE SYSTEMS AND MATHEMATICAL DESCRIPTION OF THE TORIC PART OF THE ROLLER

A. The Sets of Axis and Their Transformation

Consider three coordinate systems (see Fig. 4):

(1) (x,y,z) cartesian coordinate system, with the origin O'. The axis z is the axis of cylindrical symmetry for the roller, and the origin is the center of the toric portion of the roller.

(2) (X,Y,Z) cartesian coordinate system, with the origin O. The axis Z is the axis of cylindrical symmetry for the cone.

(3) (R,θ,Z) cylindrical polar coordinates with the same origin O and Z axis as the second cartesian system.

The directional cosines for transformation from (x,y,z) system to (X,Y,Z) system and vice versa can be represented in the following way.

Table AI - Directional Cosines

	x	y	z
X	$\cos\alpha_o$	0	$\sin\alpha_o$
Y	o	1	0
Z	$-\sin\alpha_o$	0	$\cos\alpha_o$

The transformation scheme is according to the following equation.

$$\left.\begin{aligned} x_i &= a_i + a_{ij}X_j \\ X_j &= b_j + a_{ij}x_i \end{aligned}\right\} \qquad (A1)$$

where: i = 1,2,3 denote the column number in Table AI

j = 1,2,3 denote the row number in Table AI

a_i = denote the coordinates of the origin O in the (x,y,z) coordinate system,

$a_1 = a_2 = 0$

$a_3 = -Fn$,

b_j = denote the coordinates of the origin O' in the (X,Y,Z) coordinate system,

$b_1 = Fn \sin\alpha_o$,

$b_2 = 0$,

$b_3 = Fn \cos\alpha_o$,

$x_1 = x$,

$x_2 = y$,

$x_3 = x$,

$X_1 = X$,

$X_2 = Y$, and

$X_3 = Z$.

The transformation is now getting this shape:

$$x_1 = x = a_1 + a_{11}X_1 + a_{12}X_2 + a_{13}X_3 = a_{11}X_1 + a_{13}X_3 = X\cos\alpha_o - z\sin\alpha_o$$

$$x_2 = y = a_2 + a_{21}X_1 + a_{22}X_2 + a_{23}X_3 = a_{22}X_2 = Y$$

$$x_3 = z = a_3 + a_{31}X_1 + a_{32}X_2 + a_{33}X_3 = a_3 + a_{31}X_1 + a_{33}X_3 = -Fn + X\sin\alpha_o + Z\cos\alpha_o$$

And applying the second of Equation (A1), one gets:

$$X_1 = X = x\cos\alpha_o + z\sin\alpha_o + Fn\sin\alpha_o$$

$$X_2 = Y = y$$

$$X_3 = Z = -x\sin\alpha_o + z\cos\alpha_o + Fn\cos\alpha_o$$

The transformation from R, θ Z system to (X,Y,Z) system is to be performed by:

$$X = R\cos\theta$$

$$Y = R\sin\theta$$

$$Z = Z$$

and from (X,Y,Z) to (R,θ,Z) is performed through

$$R = \sqrt{X^2 + Y^2}$$

$$\theta = \cos^{-1} \frac{X}{\sqrt{X^2+Y^2}} = \sin^{-1} \frac{Y}{\sqrt{X^2+Y^2}} = \tan^{-1} \frac{Y}{X}$$

$$Z = Z$$

The transformation from either system to any other system of the three is now given.

$$\left\{\begin{array}{l} x = X\cos\alpha_0 - Z\sin\alpha_0 = R\cos\theta\cos\alpha_0 - Z\sin\alpha_0 \\ y = Y = R\sin\theta \\ z = X\sin\alpha_0 + Z\cos\alpha_0 - Fn = R\cos\theta\sin\alpha_0 + Z\cos\alpha_0 - Fn \end{array}\right.$$

$$\left\{\begin{array}{l} X = R\cos\theta = x\cos\alpha_0 + z\sin\alpha_0 + Fn\sin\alpha_0 \\ Y = R\sin\theta = y \\ Z = Z = -x\sin\alpha_0 + z\cos\alpha_0 + Fn\cos\alpha_0 \end{array}\right. \qquad \text{(A2)}$$

$$\left\{\begin{array}{l} R = \sqrt{X^2 + Y^2} = \sqrt{(x\cos\alpha_0 + z\cos\alpha_0 + Fn\sin\alpha_0)^2 + y^2} \\ \theta = \cos^{-1} \dfrac{X}{\sqrt{X^2+Y^2}} = \sin^{-1} \dfrac{Y}{\sqrt{X^2+Y^2}} = \cos^{-1} \dfrac{x\cos\alpha_0 + z\sin\alpha_0 + Fn\sin\alpha_0}{\sqrt{(x\cos\alpha_0 + z\sin\alpha_0 + Fn\sin\alpha_0)^2 + y^2}} \\ Z = z = -x\sin\alpha_0 + z\cos\alpha_0 + Fn\cos\alpha_0 \end{array}\right.$$

B. The Roller

The roller is composed of a half torus and a cylinder.

The half torus exists for $z \geq 0$. Its equations are:

$$\left\{\begin{array}{l} \left[\sqrt{x^2 + y^2} - \rho_0\right]^2 + z^2 - r_0^2 = 0 \\ G = \left[\sqrt{(R\cos\theta\cos\alpha_0 - Z\sin\alpha_0)^2 + R^2\sin^2\theta} - \rho_0\right]^2 \\ \quad + \left[R\cos\theta\sin\alpha_0 + Z\cos\alpha_0 - Fn\right]^2 - r_0^2 = 0 \end{array}\right. \qquad \text{(A3)}$$


UNIVERSITY OF MICHIGAN
3 9015 02499 5451